An Unexpected Explanation for the Unsymmetrically Bridging Alkyne Ligand in $[W_2(\eta\text{-}C_5H_4Pr^i)_2Br_4(\mu\text{-}C_2Ph_2)]$ *

Philip Mountford
Department of Chemistry, University of Nottingham, Nottingham NG7 2RD, UK

Extended-Hückel molecular-orbital calculations have been performed for the recently reported alkyne complex $[W_2(\eta\text{-}C_5H_4Pr^i)_2Br_4(\mu\text{-}C_2Ph_2)]$, in which the $\mu\text{-}C_2Ph_2$ ligand is substantially distorted from the ideal perpendicular-bridging geometry by 26°. In contrast to other distorted μ-alkyne complexes for which the bonding has been analysed, the deviation of the alkyne ligand from perpendicularity does not arise from the anticipated second-order Jahn–Teller effect.

Ever since the synthesis and structural characterisation of $[Co_2(CO)_6(\mu\text{-}C_2Ph_2)]$ [1] the reactivity and bonding of dinuclear complexes containing an alkyne ligand bridging the two metal atoms has attracted substantial interest. In almost all of the complexes in this class the mode of co-ordination of the μ-alkyne ligand falls into one of two distinct and extreme classifications, namely either 'perpendicular' or 'parallel'. In parallel bridging alkyne complexes the projected angle (θ) of the alkyne C_{ac}–C_{ac} vector (where C_{ac} refers to the ligating carbon atom) onto the metal–metal vector is 0° (or 180°); in perpendicular bridging complexes θ is 90°. A general theoretical analysis of the bonding in parallel and perpendicular bridging alkyne complexes using the extended-Hückel method has been described by Hoffmann and co-workers.[2]

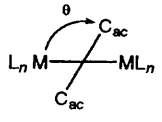

For many μ-alkyne complexes small deviations in θ from the ideal values of either 90 or 0° are observed,[3] but these have generally been attributed to steric or crystal-packing effects. However, several μ-alkyne binuclear complexes have been described which show such substantial deviations of the μ-alkyne ligand from either of the two ideal orientations that some effort has been spent in both seeking and proving an alternative (orbital) explanation. For the complexes $[W_2Cl_4(\mu\text{-}NMe_2)_2(\mu\text{-}C_2Me_2)(py)_2]$ (py = pyridine) (θ = 55°),[4a] $[Co_2(CO)_2(\mu\text{-dppm})_2(\mu\text{-}C_2Me_2)][PF_6]$ (dppm = $Ph_2PCH_2PPh_2$) (θ = 79°),[4b] and $[Nb_2Cl_4O(\mu\text{-}C_2Ph_2)(thf)_4]$ (thf = tetrahydrofuran) (θ = 59°)[4c] the alkyne distortion has been successfully rationalised using extended-Hückel molecular orbital (EHMO) calculations (for the W_2 and Co_2 complexes) and/or the SCF-Xα-SW method (for the W_2 and Nb_2 species).[5–7] In all of these complexes the deviation of the μ-alkyne ligand from the ideal perpendicular bridging geometry (θ = 90°) has been very clearly identified as a second-order Jahn–Teller effect.[8] Cotton and Feng[7] have proposed that this explanation of substantially distorted μ-alkyne complexes has a general validity.

Other complexes[9] also have large deviations of a μ-alkyne ligand namely $[(Me_2NCS)(\eta^2\text{-}Me_2NCS_2)W(\mu\text{-}S)\{\mu\text{-}C_2(NMe_2)_2\}WS\{S_2Sn[CH(SiMe_3)_2]_2\}]$ (θ = 55°) and $[(\eta^2\text{-}C_2Et_2)ORe(\mu\text{-}O)(\mu\text{-}C_2Et_2)Re(\eta^2\text{-}C_2Et_2)_2]$ (θ = 56°) but the bonding in these highly asymmetric molecules has not yet been analysed.

* *Non-SI unit employed:* eV ≈ 1.60 × 10^{-19} J.

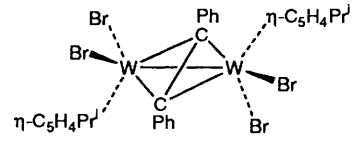

1

As part of a systematic study of the W≡W triply bonded complexes $[W_2(\eta\text{-}C_5H_4R)_2X_4]$ (X = Cl or Br), Green and co-workers[10] prepared the μ-alkyne complex $[W_2(\eta\text{-}C_5H_4Pr^i)_2Br_4(\mu\text{-}C_2Ph_2)]$ **1**. The synthesis and crystal structure determination of **1** has been described elsewhere.[11] Compound **1** contains a bridging diphenylacetylene ligand rotated by 26° from the ideal perpendicular bridging geometry (*i.e.* θ = 64 or 116°).

As a continuation of previous studies of potentially second-order Jahn–Teller distorted μ-alkyne complexes,[12] it was of interest to see whether the structure of **1** could be rationalised in this way using EHMO calculations.[13] In addition, the geometry of the $W_2(\eta\text{-}C_5H_4Pr^i)_2Br_4$ fragment in **1** is intriguing as it contains eclipsed $\eta\text{-}C_5H_4Pr^i$ and Br ligands *trans* to the μ-C_2Ph_2 ligand whereas the Br ligands *cis* to the alkyne bridge are not eclipsed. The origins of this unusual $W_2(\eta\text{-}C_5H_4Pr^i)_2Br_4$ fragment geometry and its relationship to the distortion of the μ-alkyne ligand are now explained.

Calculations and Discussion

In order to simplify the analysis of the bonding in $[W_2(\eta\text{-}C_5H_4Pr^i)_2Br_4(\mu\text{-}C_2Ph_2)]$ **1** a series of model complexes was studied having the basic formula $[W_2(\eta\text{-}C_5H_5)_2Br_4(\mu\text{-}C_2H_2)]$ with structural parameters based around those of **1** and idealised to C_2 symmetry. The fragment-analysis approach is a straightforward way of understanding the interaction of an alkyne with a dimetal centre[2] and here the $[W_2(\eta\text{-}C_5H_5)_2Br_4(\mu\text{-}C_2H_2)]$ model is imagined to be assembled from $W_2(\eta\text{-}C_5H_5)_2Br_4$ and μ-C_2H_2 fragments. This method allows the separation of the bonding characteristics and stereochemical preferences of the two moieties. Once the basic features of the $W_2(\eta\text{-}C_5H_5)_2Br_4$ fragment and $W_2(\eta\text{-}C_5H_5)_2Br_4$–μ-alkyne bonding have been identified we shall be able to find the reason for the distortion in the μ-alkyne bridge.

The μ-C_2H_2 *Fragment.*—The derivation and nature of the frontier orbitals of *cis* bent C_2H_2, which are shown on the right of Figs. 1 and 2, have been described in detail elsewhere.[2,14] They transform as (in increasing order of stability) $a_2 + b_1 + a_1 + b_2$ under the C_{2v} symmetry of the fragment {and simply

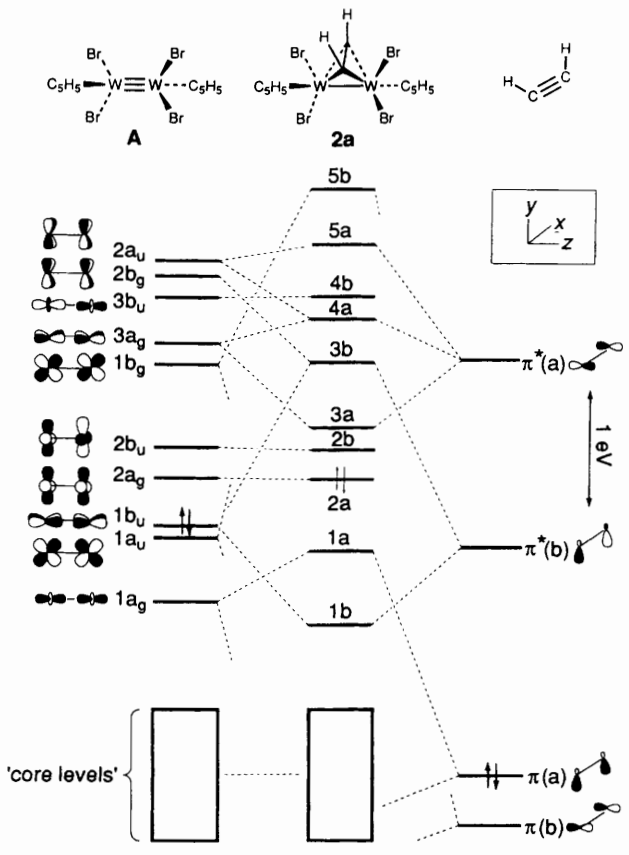

Fig. 1 Interaction diagram for staggered $W_2(\eta\text{-}C_5H_5)_2Br_4$ **A** with *cis*-C_2H_2 to give $[W_2(\eta\text{-}C_5H_5)_2Br_4(\mu\text{-}C_2H_2)]$ **2a**. The highest occupied molecular orbital (HOMO) in each fragment and in the resultant complex is indicated by double arrows

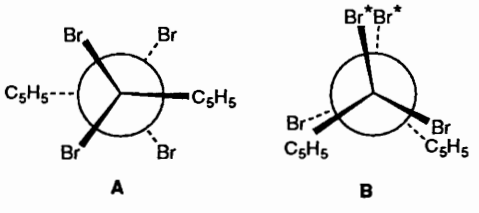

as a + b + a + b under the C_2 symmetry of $[W_2(\eta\text{-}C_5H_5)_2Br_4(\mu\text{-}C_2H_2)]$}. For convenience, they will be referred to herein as (in increasing order of stability) π*(a), π*(b), π(a) and π(b).

The $W_2(\eta\text{-}C_5H_5)_2Br_4$ *Fragment.*—The $W_2(\eta\text{-}C_5H_5)_2Br_4$ unit may adopt one of two idealised conformations while keeping a minimum separation between the C_5H_5 rings on the adjacent metals. These are the staggered (C_{2h}, **A**) or eclipsed (C_2, **B**) conformers shown in Newman projection. In the eclipsed geometry the bromide ligands which are mutually eclipsed are labelled Br* for ease of future reference.

An EHMO bonding study for staggered $[W_2(\eta\text{-}C_5H_5)_2Cl_4]$, the chloride analogue of **A**, has been previously described. The calculations were backed up by He I and He II gas-phase photoelectron and solution UV/VIS spectra for the real complex $[W_2(\eta\text{-}C_5H_4Pr^i)_2Cl_4]$ [W≡W 2.3678(6) Å].[10a,15]

According to the calculations reported here the level ordering of the frontier orbitals of staggered $W_2(\eta\text{-}C_5H_5)_2Br_4$ (**A**, shown at the left in Fig. 1) is almost identical to that found for the chloride analogue,[15] except that the orbital splittings are less at the longer W–W separation (2.80 Å) employed here. The $W_2(\eta\text{-}C_5H_5)_2Br_4$ fragment contains a W≡W triple bond

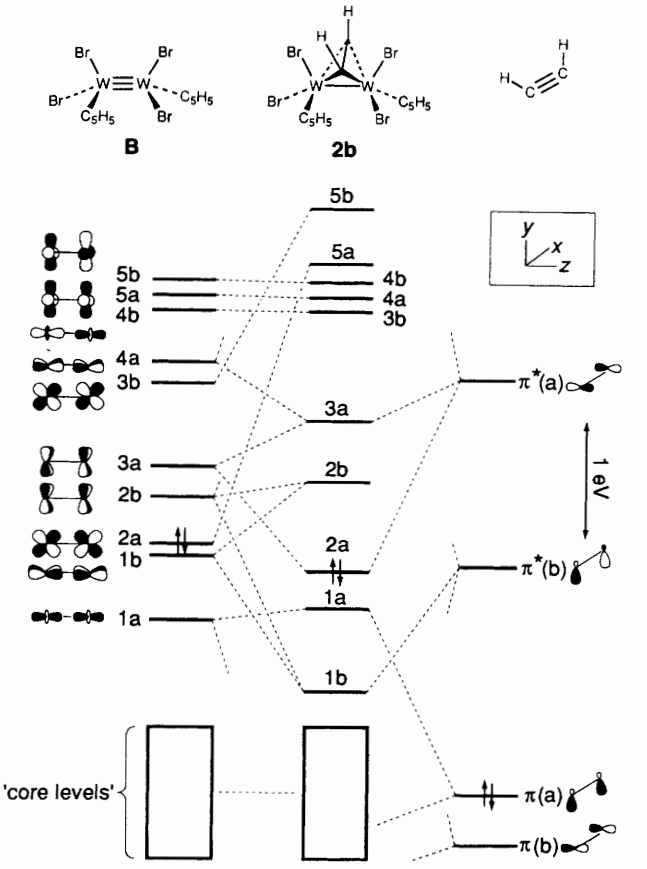

Fig. 2 Interaction diagram for eclipsed $W_2(\eta\text{-}C_5H_5)_2Br_4$ **B** with *cis*-C_2H_2 to give $[W_2(\eta\text{-}C_5H_5)_2Br_4(\mu\text{-}C_2H_2)]$ **2b**. The HOMO in each fragment and in the resultant complex is indicated by double arrows

of configuration $\sigma(d_{z^2})^2\ \pi(d_{yz})^2\ \pi(d_{xz})^2$.† The $\delta(d_{x^2-y^2})$ and $\delta^*(d_{x^2-y^2})$ combinations form the lowest unoccupied molecular orbital (LUMO) ($2a_g$) and next lowest unoccupied molecular orbital ($2b_u$) respectively. The remaining d-orbital combinations, $\delta(d_{xy})$ and $\delta^*(d_{xy})$ ($2b_g$ and $2a_u$ respectively), are pushed high up in energy due to strong interactions with the C_5H_5 and Br ligand set.

A nearly equivalent description of the d^3–d^3 manifold is found for the eclipsed C_2 rotamer **B** the frontier orbitals of which are shown at the left in Fig. 2. The most important consequence (from the point of view of W_2–alkyne bonding) of the eclipsing of the two $W(\eta\text{-}C_5H_5)Br_2$ units on passing from **A** to **B** is the dramatic stabilisation of the $\delta(d_{xy})$ and $\delta^*(d_{xy})$ orbital combinations which now find a much poorer match with the ligand set and so form the major contributions to the LUMO (2b) and next lowest unoccupied molecular orbital (3a) in **B**. Conversely, the $\delta(d_{x^2-y^2})$ and $\delta^*(d_{x^2-y^2})$ combinations find a better match with the ligand set and are raised high in energy. Note that in **B** we cannot completely separate (*i.e.* by symmetry) the two types of δ or δ* combinations and there is some contribution from $\delta^*(d_{x^2-y^2})$ in 2b and from $\delta(d_{x^2-y^2})$ in 3a [that $\delta(d_{x^2-y^2})$ and $\delta^*(d_{xy})$ can mix in this way becomes critically important later on]. The transformation from staggered to eclipsed $W_2(\eta\text{-}C_5H_5)_2Br_4$ has little effect on the orbital energies of the d^3–d^3 manifold and the reduced metal–metal overlap population (Table 1). Total computed (sum

† Although the symmetries of the species under consideration here are much lower than cylindrical, the classification of orbitals according to the σ, π and δ notation is nevertheless a useful distinction based on predominant orbital type, and gives an easy comparison with other metal–metal bonded systems. In order to preserve the usual choice of atomic orbitals for metal–metal bonding the *y* axis was chosen as the principal axis for the fragments and molecules.

Table 1 Mulliken overlap and orbital populations for the model complexes and fragments

Model or fragment	Overlap population				Orbital population				Net alkyne charge
	C_{ac}–C_{ac}	W–W	W–C_{ac}	W–C_{ac}	π(b)	π(a)	π*(b)	π*(a)	
cis bent C_2H_2	1.56	—	—	—	2.00	2.00	0.00	0.00	0.00
A	—	0.75	—	—	—	—	—	—	—
B	—	0.75	—	—	—	—	—	—	—
2a	1.17	0.44	0.24	0.31	1.60	1.78	1.05	0.26	−0.62
2b	1.01	0.34	0.36	0.36	1.63	1.79	1.13	0.82	−1.27
2c	1.01	0.33	0.36	0.36	1.64	1.79	1.10	0.84	−1.27
2d	1.05	0.39	0.29	0.40	1.61	1.78	1.09	0.65	−1.04
2e	1.05	0.43	0.13	0.60	1.62	1.73	1.11	0.61	−0.95

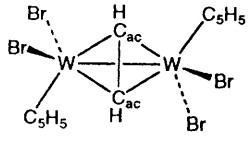

2a

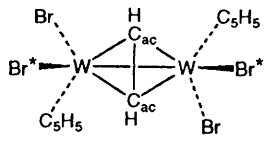

2b

W-W-Br* 101.5°

of one-electron) energies, however, indicate a preference of *ca.* 1.2 eV for the staggered geometry **A** even at this relatively long W–W separation. The differences in total energies between **A** and **B** set the geometrical preferences of the *isolated* $W_2(\eta\text{-}C_5H_5)_2Br_4$ fragment for the staggered geometry.

$W_2(\eta\text{-}C_5H_5)_2Br_4$–*Alkyne Bonding*.—The result of allowing *cis* bent C_2H_2 to interact with staggered $W_2(\eta\text{-}C_5H_5)_2Br_4$ **A** to give the μ-alkyne complex **2a** is shown at the centre in Fig. 1. Important Mulliken orbital and overlap populations are listed in Table 1.

In the complex **2a** only three of the four frontier orbitals of C_2H_2 are involved to any significant extent in metal–alkyne bonding. The bonding combination (3a) of the alkyne π*(a) level with the metal δ*(d_{xy}) ($2a_u$) level is vacant according to the calculations. Hence the Mulliken population of the π*(a) fragment orbital in **2a** is much less than that of π*(b) (see Table 1). The three highest-occupied orbitals of **2a** are predominantly metal-based, metal–metal-bonding combinations and so the tungsten–tungsten interaction in this complex may still be *formally* described as a W≡W triple bond.

Consider now the interaction of C_2H_2 with eclipsed $W_2(\eta\text{-}C_5H_5)_2Br_4$ **B** to give the eclipsed μ-alkyne complex $[W_2(\eta\text{-}C_5H_5)_2Br_4(\mu\text{-}C_2H_2)]$ **2b**. The resultant level ordering for this complex is shown at the centre in Fig. 2 and immediately we can see that both pairs of alkyne π and π* levels are now involved in metal–alkyne bonding. Owing to the lowering in energy of the $W_2(\eta\text{-}C_5H_5)_2Br_4$ fragment δ*(d_{xy}) level (*i.e.* 3a in **B**), the HOMO (2a) in **2b** is now the bonding combination between this metal–metal antibonding orbital and the alkyne π*(a) level. The computed net stabilisation on going from **2a** to **2b** is *ca.* −3 eV, much of which can be traced to the stabilisation of the 1b and 2a orbitals, both active in metal–alkyne back bonding. Of the occupied frontier orbitals of **2b** only 1a [σ(d_{z^2})] has substantial W_2 character (84%) and represents the main direct metal–metal bonding interaction. Table 1 shows that the enhanced metal-to-alkyne back bonding is reflected in the C_2H_2 fragment π*-orbital populations and increased net alkyne negative charge. Since in **2b** the 1b and 2a levels are predominantly ligand-based and represent strong $W_2 \rightarrow C_2$ π donation, the occupancies and nature of the frontier orbitals of **2b** are consistent with its having a *formal* W–W single bond and a $[C_2H_2]^{4-}$ ligand.

In summary, we ought to expect the $W_2(\eta\text{-}C_5H_5)_2Br_4$ fragment in $[W_2(\eta\text{-}C_5H_5)_2Br_4(\mu\text{-}C_2H_2)]$ to favour strongly an eclipsed geometry **2b**. The preference of the isolated $W_2(\eta\text{-}C_5H_5)_2Br_4$ units on their own for a staggered geometry **A** is overwhelmed by the energetic benefits of enhanced metal-to-alkyne π donation in **2b**.

Further Stereochemical Preferences of the $W_2(\eta\text{-}C_5H_5)_2Br_4$ *Fragment*.—In the crystallographically characterised complex $[W_2(\eta\text{-}C_5H_4Pr^i)_2Cl_4]$ the four W–W–Cl angles are equal within experimental error.[10a] In order to understand the basic preferences of the model complexes their geometries were idealised so that the four W–W–Br angles were identical. In the real compound $[W_2(\eta\text{-}C_5H_4Pr^i)_2Br_4(\mu\text{-}C_2Ph_2)]$ the bromide ligands *cis* to the $\mu\text{-}C_2Ph_2$ ligand are bent back further (W–W–Br ≈ 122°) and those *trans* to it (W–W–Br ≈ 100.5°), presumably due to the steric influence of the bridging C_2Ph_2 ligand (which is shown below to be a valid supposition). Also, while the Br and $\eta\text{-}C_5H_4Pr^i$ ligands *trans* to the alkyne ligand are mutually eclipsed as anticipated from calculations on **2a** and **2b**, the bromide ligands *cis* to the alkyne are displaced to either side of the plane containing the W–W vector and centre of the C_{ac}–C_{ac} bond so that they are related by a dihedral angle Br–W–W–Br of 62.9°.

From the calculations for complexes **2a** and **2b** the basic geometrical requirement of the $W_2(\eta\text{-}C_5H_5)_2Br_4$ fragment for most effective metal–alkyne bonding was found (*i.e.* **2b**, fully eclipsed). In order to discuss the reasons for the movement of the bromide ligands in **1** out of the plane containing the W–W bond we need to introduce the dihedral angle φ = Br*–W–W–Br* (recall that the bromide ligands labelled Br* are those which are mutually eclipsed in **B** and **2b** *i.e.* when φ = 0°).

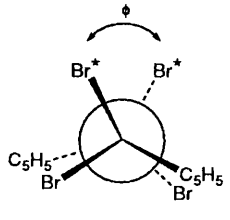

Starting with fully eclipsed fragment $W_2(\eta\text{-}C_5H_5)_2Br_4$ **B**, it was found that as the W–W–Br* angle was increased from 100.5 to 122° the Br* atoms moved closer to the neighbouring C_5H_5 ligands. For the angles W–W–Br set *equal* to W–W–Br* in **B**, increasing the dihedral angle φ leads only to a steady increase in the total computed energy (a net destabilisation). However, for W–W–Br 100.5, W–W–Br* 122° a minimum in the total energy of *ca.* −2.8 eV (relative to φ = 0°) was found for φ = 56°. This computed φ value compares well to that found in the crystal structure of **1** (62.9°). Furthermore, the value of φ of the minimum-energy geometry decreases with decreasing angle W–W–Br*, finally arriving back at φ = 0° for W–W–Br = W–W–Br*.

These results suggest that a large antibonding interaction (steric repulsion) between Br* and the proximal C_5H_5 group is turned on as the angle W–W–Br* is increased and that it is this

factor which is responsible for setting the dihedral angle, φ. That an approximately correct value of φ is found in the *absence* of a μ-C_2H_2 ligand in **B** suggests that the deviation of the $W_2(\eta\text{-}C_5H_4Pr^i)_2Br_4$ fragment geometry from eclipsed in complex **1** is caused only by the steric bulk of the bridging ligand, the preferred geometry for optimum metal–alkyne bonding being the fully eclipsed one.

Alkyne Rotation in $[W_2(\eta\text{-}C_5H_5)_2Br_4(\mu\text{-}C_2H_2)]$.—The calculations for $[W_2(\eta\text{-}C_5H_5)_2Br_4(\mu\text{-}C_2H_2)]$ were repeated using the experimentally determined W–W–Br* value (*i.e.* increasing from 100.5 to 122°) while keeping the fully eclipsed $W_2(\eta\text{-}C_5H_5)_2Br_4$ core (φ = 0°). The frontier-level ordering for this complex **2c** is shown at the left in Fig. 3 and is essentially unchanged from that presented in Fig. 2 for **2b** with the exception that two levels (labelled Br* in Fig. 3) have risen out of the core and now lie above **1b**. They contain large contributions from the lone pairs on the Br* ligands and have been pushed up in energy because the separation between Br* and C_5H_5 has decreased on increasing the angle W–W–Br*. The increase in the W–W–Br* angle has a negligible effect on the overlap or orbital populations listed in Table 1, but does destabilise the complex by *ca.* 2.5 eV [as anticipated above by the calculations on the $W_2(\eta\text{-}C_5H_5)_2Br_4$ fragment]. That the numerical quantities in Table 1 and energies of the metal–alkyne bonding orbitals (Figs. 2 and 3) are essentially unaffected by increasing W–W–Br* supports the view that the bending back of the Br* ligands is a steric effect alone.

To the centre and right of Fig. 3 are the level orderings for two new models **2d** and **2e** in which two successive changes have been made. First of all the dihedral angle φ is increased to 63° (**2c** ⟶ **2d**) and then the alkyne is rotated about the C_2 symmetry axis by 26° (**2d** ⟶ **2e**). The model **2e** represents the geometry found in the crystal structure of **1**. Model **2d** is identical to **2e** except that the alkyne has not yet been allowed to rotate and is a 'half-way house' between the fully eclipsed core of **2c** and the crystallographically determined geometry **2e**.

The total energy curve for model **2d** as φ is changed reveals a well located minimum at around φ = 60°. This value is reassuringly close to that found in complex **1**, and is also consistent with the calculations on the $W_2(\eta\text{-}C_5H_5)_2Br_4$ fragment alone (see above). One of the most obvious changes on passing from **2c** to **2d** is the stabilisation of the Br* lone-pair level (an overall net stabilisation of *ca.* −3 eV accompanies the transition from **2c** to **2d**).

The calculations very successfully reproduce the geometry of the $W_2(\eta\text{-}C_5H_4Pr^i)_2Br_4$ moiety in complex **1**; do they also predict a distortion of the μ-alkyne ligand (in the model complexes **2d** ⟶ **2e**)? When the alkyne ligand in **2d** was allowed to rotate by 26° (giving **2e**) a net stabilisation of −0.75 eV was found, −0.64 eV of which may be traced to the behaviour of the two highest-occupied molecular orbitals (1a and 2a). So the computational method and models are valid, the correct answer is found. However, to *understand* properly the rotation of the alkyne we need to examine the individual steps **2c** ⟶ **2d** and then **2d** ⟶ **2e** in more detail.

Model **2c** *to* **2d**. Table 1 shows that when φ is increased to 63° (**2c** ⟶ **2d**) the extent of metal–alkyne bonding is diminished [shown by increases in the C_{ac}–C_{ac} and W–W reduced overlap populations and also by a reduction in net alkyne charge, the main contribution here being a decrease in the π*(a) Mulliken population]. Additionally, the asymmetry in the individual W–C_{ac} net overlap populations for model **2d** (which are equal to each other in **2c**) indicates a tension in the perpendicular bridging $W_2(\mu\text{-}C_2H_2)$ sub-unit and this alone suggests that a distortion may be expected.

Fig. 3 shows that the 1a and 2a levels (the two highest-occupied molecular orbitals) are destabilised, and the 3a level is stabilised on increasing φ. This arises partly because the 1a and 2a levels of models **2b** and **2c** contain δ*(d_{xy})–π*(a) bonding character (see Fig. 2) whereas 3a contains δ*(d_{xy})–π*(a)

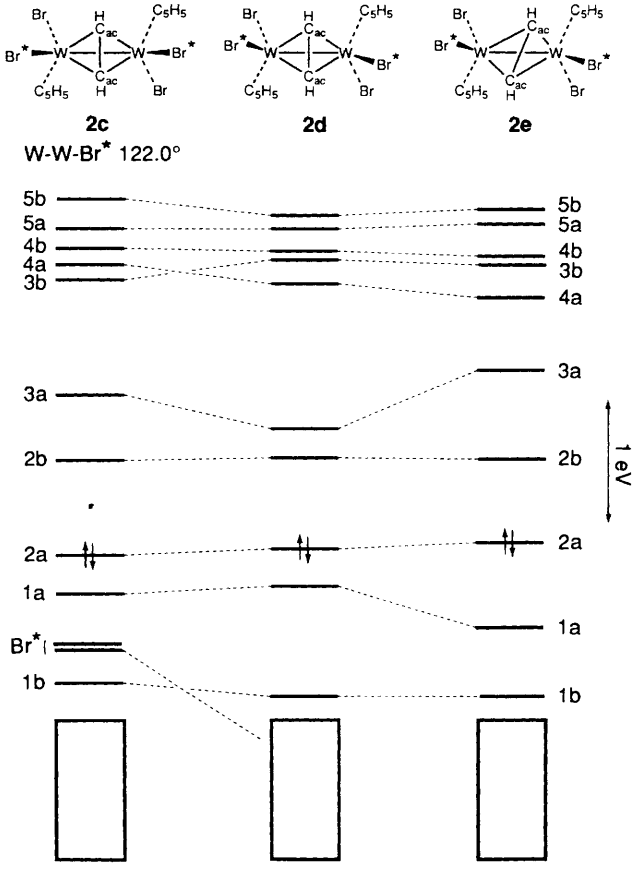

Fig. 3 Walsh diagram for **2c** ⟶ **2d** ⟶ **2e** (see text for details). The HOMO in each fragment and in the resultant complex is indicated by double arrows

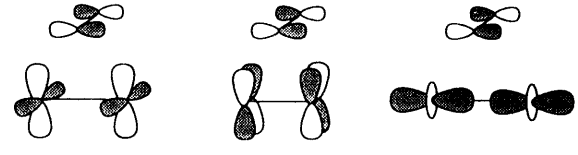

I II III

antibonding character. As φ increases (**2c** ⟶ **2d**) the Br* ligands move off the angular nodes of the W d_{xy} atomic orbitals and at the same time move toward the angular nodes of the W $d_{x^2-y^2}$ levels. The d_{xy} atomic orbitals are partly diverted to W–Br* bonding interactions and more $d_{x^2-y^2}$ character is available. The result is that the relative contribution of δ($d_{x^2-y^2}$) to 1a, 2a and 3a increases and that from δ*(d_{xy}) decreases. For example, the calculations reveal that the process **2c** ⟶ **2d** results in a decrease of δ*(d_{xy}) character in the HOMO (2a) from 59 (in **2c**) to 39% (in **2d**); the δ($d_{x^2-y^2}$) character meanwhile increases from 7 (in the HOMO of **2c**) to 32% (in **2d**). Similar changes in the relative contributions of δ*(d_{xy}) and δ($d_{x^2-y^2}$) to 1a and 3a are also found. Therefore, we essentially have in **2d** a situation that is intermediate between the staggered and eclipsed μ-alkyne models **2a** and **2b**.

In the perpendicular bridging geometry the alkyne π*(a) level has no net overlap with the δ($d_{x^2-y^2}$) combination (as illustrated by **I**) even though they have the same symmetry labels. Therefore the level energetics in Fig. 3 register only the loss of overlap with δ*(d_{xy}) (illustrated by **II**); the same explanation accounts for the changes in W–W and C_{ac}–C_{ac} overlap populations, the decrease in the Mulliken orbital population of π*(a) and the diminished net alkyne negative charge in model **2d** as compared to **2c** (Table 1).

Model **2d** *to* **2e**. Model **2d** is the perpendicular bridging equivalent of the final destination, **2e**. We know (from the total energies) that **2d** is unstable with respect to distortion involving rotation of the μ-C_2H_2 ligand. However, before looking at the alkyne rotation in **2d**, we ought to look at rotation in the more symmetrical case, **2c**, to see if the enablement of the alkyne rotation depends on the bending of the Br* ligands out of the vertical plane containing the W_2 unit, *i.e.* on increasing φ.

When the alkyne was rotated in the fully eclipsed complex **2c** ($\varphi = 0°$ and W–W–Br* 122°) only a steady net destabilisation was found in both the total energies and the sum of the energies of the three occupied frontier orbitals (1b, 1a, 2a). The 1a and 2a levels strongly repel each other, with the latter climbing rapidly in energy and the former stabilising as alkyne rotation proceeds (the energy of 1b changes relatively little compared with those of 1a and 2a). The 2a level is destabilised because of loss of bonding overlap of $\delta^*(d_{xy})$ with $\pi^*(a)$ (shown for $\theta = 90°$ in **II**) on rotation away from $\theta = 90°$. The 1a (σ-bonding level) is stabilised mainly by development of bonding overlap of the d_{z^2} tungsten orbitals with the alkyne $\pi^*(a)$ level (see **III**) among others [under the low C_2 symmetry, 1a contains contributions also from metal $\delta(d_{x^2-y^2})$ and $\pi(d_{yz})$ combinations which can also develop non-zero overlaps with $\pi^*(a)$ on alkyne rotation]. Since the 2a [$\delta^*(d_{xy})$–alkyne $\pi^*(a)$ bonding] level is occupied, net destabilisation of the 1a/2a manifold results. *No alkyne rotation is predicted at* $\varphi = 0$.

In contrast, when the alkyne moiety was allowed to rotate in model **2d** (*i.e.* **2d** ⟶ **2e**, Fig. 3) again the 1a level was substantially stabilised and the 3a destabilised, but the 2a level (HOMO) was only destabilised by *a relatively small amount* (+0.08 eV at $\varphi = 63°$ compared to +0.40 eV for the same rotation in the fully eclipsed **2c**). Moreover, a large net stabilisation of −0.75 eV is found on going from **2d** to **2e**, most of which comes from the stabilisation of the 1a orbital. To check for the effects of direct repulsion between the Br* and C_{ac} atoms, the calculations were repeated for **2d** and **2e** with all the overlaps $\langle C_{ac}|Br^*\rangle$ set to zero. The stabilisation persisted, and again was largely attributable to the large stabilisation of the 1a orbital, with the 2a orbitals being only slightly destabilised. Clearly it is predominantly the behaviour of the 2a level in **2c** and **2d** on alkyne rotation that controls whether or not rotation of the alkyne occurs. What is the reason for the differing behaviour of the 2a orbital towards alkyne rotation in the two models **2c** and **2d**?

The answer to this question lies in the amount of $\delta^*(d_{xy})$ and $\delta(d_{x^2-y^2})$ character in the 2a orbital in models **2c** and **2d**. As described above, in the fully eclipsed **2c** the tungsten contribution to 2a contains eight times as much $\delta^*(d_{xy})$ as $\delta(d_{x^2-y^2})$ character. In **2d**, however, the contributions from the $\delta^*(d_{xy})$ and $\delta(d_{x^2-y^2})$ combinations are approximately equal. For $\theta = 90°$ (perpendicular bridge) the value of the integral $\langle\delta(d_{x^2-y^2})|\pi^*(a)\rangle$ is zero due to nodal plane mismatch (see **I**). Conversely, $\langle\delta^*(d_{xy})|\pi^*(a)\rangle$ is maximised (see **II**). As alkyne rotation proceeds, $\langle\delta^*(d_{xy})|\pi^*(a)\rangle$ decreases and $\langle\delta(d_{x^2-y^2})|\pi^*(a)\rangle$ [and $\langle\sigma(d_{z^2})|\pi^*(a)\rangle$] increases. The smaller the contribution from $\delta^*(d_{xy})$ to 2a, the less the orbital will be destabilised on alkyne rotation; similarly, the greater the contribution from $\delta(d_{x^2-y^2})$ to 2a, the more the orbital will be stabilised on twisting. Thus in **2c** [where 2a possesses little $\delta(d_{x^2-y^2})$ character] alkyne rotation leads mainly to loss of $\pi^*(a)$–$\delta^*(d_{xy})$ bonding and so 2a rises substantially in energy. In **2d** [where 2a possesses comparable $\delta(d_{x^2-y^2})$ character] loss of overlap between $\pi^*(a)$ and $\delta^*(d_{xy})$ is partially compensated by the increase in $\pi^*(a)$–$\delta(d_{x^2-y^2})$ bonding so the orbital stays fairly low in energy.

The latter effect was tested by repeating the calculations for models **2d** and **2e** with the overlaps between the components of $\delta(d_{x^2-y^2})$ and $\pi^*(a)$ deleted. For **2d** there was, as expected, only a slight change in the energies of the frontier orbitals and in the overall computed energy of the complex. For **2e** there was a large destabilisation of orbital 2a relative to the previous calculation for **2e** (where all overlaps were included) and an overall destabilisation on alkyne rotation.

Finally, there are, of course, other interactions with $\pi^*(a)$ that come into play on alkyne rotation [*e.g.* non-zero overlap with the $\pi(d_{yz})$ bonding level] and these also change in magnitude with increasing φ. The interaction with $\delta(d_{x^2-y^2})$ is the most important one according to these calculations.

Comparison of the Origin of Alkyne Rotation in Complex **1** *with that for Other Distorted* μ*-Alkyne Systems.*—Let us see how the origin of the alkyne rotation for **1** compares with the explanations offered for other substantially distorted alkyne complexes. Recall that other complexes in which the μ-alkyne ligand deviates considerably from perpendicularity include $[W_2Cl_4(\mu\text{-}NMe_2)_2(\mu\text{-}C_2Me_2)(py)_2]$ ($\theta = 55°$),[4a] $[Co_2(CO)_2(\mu\text{-dppm})_2(\mu\text{-}C_2Me_2)][PF_6]$ ($\theta = 79°$),[4b] and $[Nb_2Cl_4O(\mu\text{-}C_2Ph_2)(thf)_4]$ ($\theta = 59°$).[4c] Calculations using the EHMO[5,6] and/or the SCF-Xα-SW method[7] have been carried out on appropriate model complexes. The approach of previous workers has been to put the alkyne back into the ideal perpendicular-bridging position and then to identify the driving force for rotation. I have already used this device in the analysis of the alkyne rotation on going from model **2d** to **2e**.

The previous results may be summarised thus:[5–7] (*i*) all the calculations so far carried out on distorted alkyne complexes with the alkyne placed back in the ideal perpendicular-bridging geometry found a very small (< 0.2 eV) HOMO–LUMO gap (for the cationic Co_2 complex the small energy gap is between a filled and half-filled level but the same arguments apply); (*ii*) all the calculations found the HOMO to be a metal–metal bonding combination (of a_1 symmetry under C_{2v}) with the low-lying LUMO (or half-occupied orbital for the Co_2 case) being a M_2–$\pi^*(a)$ bonding combination (transforming as a_2 under C_{2v}). The dimetal–alkyne $\pi^*(a)$ bonding level is therefore either essentially unoccupied or half-occupied in the perpendicular-bridging geometries in all these complexes.

In a molecule where there is a small energy gap between a HOMO of one symmetry label and a LUMO having another a second-order Jahn–Teller distortion is usually anticipated.[8] For a second-order Jahn–Teller distortion to occur at all the distortion must be of the correct symmetry to allow intermixing between the two orbitals in question, and for the distortion to be significant the interacting orbitals must lie very close together in energy in the non-distorted geometry.

As stated, in the distorted alkyne complexes previously studied there is a small HOMO–LUMO gap in the non-distorted geometry. Secondly, alkyne rotation is of a_2 symmetry (in the C_{2v} point group) and this allows a second-order Jahn–Teller distortion since $\Gamma_{HOMO} \times \Gamma_{alkyne\ rotation} \times \Gamma_{LUMO}$ contains the totally symmetric representation ($a_1 \times a_2 \times a_2 = a_1$). In other words, as the alkyne rotates the HOMO and LUMO can mix and so one (the HOMO) is stabilised and the other (the LUMO, or for the Co_2 complex a half-occupied orbital) is destabilised. In orbital terms the M_2–$\pi^*(a)$ overlap (a_2) decreases on alkyne rotation whereas the overlap of the $\pi^*(a)$ alkyne orbital with the metal–metal bonding level (a_1) increases.

Even in the real complexes (for the Nb_2 and W_2 cases) where the perpendicular-bridging molecular symmetry is lower than C_{2v} (and so the HOMO and LUMO have the same symmetry labels even in the ideal perpendicular-bridging geometry) the fundamental instability of the perpendicular-bridging geometry and the mechanism for relieving the instability remain. There is a very small HOMO – LUMO gap and, owing to the nodal properties of the vacant M_2–$\pi^*(a)$ orbital and the occupied metal–metal bonding combination, no overlap is possible between these orbitals in the perpendicular-bridging geometry; rotation allows their intermixing, stabilising the HOMO and destablising the LUMO. It is still fair to call this mechanism (in spirit at least) a second-order Jahn–Teller effect.

Hence it has quite reasonably been proposed that these results might have a general validity and that they show that 'a large deviation of a bridging alkyne from perpendicularity... is due to a small HOMO – LUMO gap (with the perpendicular geometry) from which a second-order Jahn–Teller effect arises'.[7] However, there appears to be little in common between the principal features of the bonding in model **2d** and those features of the W_2, Nb_2 and Co_2 perpendicular-bridging geometries that are considered to be essential for alkyne rotation to be enabled.

Thus (*i*) model **2d** possesses a very reasonable computed HOMO – LUMO gap (0.75 eV), and, just as importantly, the HOMO and LUMO have the symmetry labels a and b so even alkyne rotation will not enable them to mix. There is a larger gap still (0.95 eV) between the HOMO and the next lowest-unoccupied molecular orbital (3a); (*ii*) the metal-based level containing the main metal $\delta^*(d_{xy})$–alkyne $\pi^*(a)$ bonding interaction is an occupied HOMO, and not a low-lying LUMO as found for the W_2, Nb_2 and Co_2 (actually half-filled) perpendicular-bridge model complexes (it is vitally important that this orbital is partially or completely unoccupied in the W_2, Co_2 and Nb_2 complexes since it is considerably destabilised on alkyne rotation). These bonding characteristics of **2d** are in fact typical of computed orbital results for distortion-free perpendicular-bridging alkyne complexes[2,12,14] where the usual features of M_2–μ-alkyne bonding include a reasonable HOMO – LUMO gap and a stable filled M_2–$\pi^*(a)$ bonding level. Clearly the bonding analysis of $[W_2(\eta\text{-}C_5H_4Pr^i)_2Br_4(\mu\text{-}C_2Ph_2)]$ (*via* model **2d**) cannot be made to fit either qualitatively or quantitatively into the general explanation offered for the second-order Jahn–Teller distorted complexes $[W_2Cl_4(\mu\text{-}NMe_2)_2(\mu\text{-}C_2Me_2)(py)_2]$, $[Co_2(CO)_2(\mu\text{-dppm})_2(\mu\text{-}C_2Me_2)][PF_6]$ or $[Nb_2Cl_4O(\mu\text{-}C_2Ph_2)(thf)_4]$.

Common Themes.—There is, fortunately, a common link between complex **1** and all of these other rotationally unstable μ-alkyne complexes. Recall that when the possibility of alkyne rotation in model **2c** was examined a rapid destabilisation of the filled 2a $\delta^*(d_{xy})$–$\pi^*(a)$ level was found on moving away from $\theta = 90°$. This inhibited the rotation even though the 1a W–W σ-bonding level was considerably stabilised along the distortion coordinate. In model **2d**, however, the diminished $\delta^*(d_{xy})$ character and increased $\delta(d_{x^2-y^2})$ character of 2a allowed rotation to occur because this level remained low in energy along the distortion coordinate; the 'brake' on distortion had been released.

In most of the perpendicular-bridge complexes for which the bonding has been analysed there exists a stable, filled M_2–$\pi^*(a)$ bonding level which helps to resist alkyne rotation.[2,12,14] In the second-order Jahn–Teller distorted alkyne complexes the M_2–$\pi^*(a)$ bonding level is either vacant or half-occupied and again the brake on the distortion is released (the rise in energy of this orbital becomes of lesser importance). The effectiveness of M ⟶ $\pi^*(a)$ back bonding is therefore an extremely important factor in preserving the perpendicular nature of the $M_2(C_2R_2)$ unit. The second-order Jahn–Teller distortion is certainly one example of how a complex takes advantage of diminished M ⟶ $\pi^*(a)$ back bonding.

The compound analysed in this contribution represents another example of the following *general phenomenon:* if there is little M ⟶ $\pi^*(a)$ back bonding to lose by rotation [the M_2–$\pi^*(a)$ bonding level is either partly or wholly unoccupied or of otherwise reduced bonding character] then a distortion driven by stabilisation of lower occupied levels is more likely to occur.

Conclusion

The deviation of the bridging alkyne in $[W_2(\eta\text{-}C_5H_4Pr^i)_2Br_4(\mu\text{-}C_2Ph_2)]$ **1** from perpendicularity is not caused by the second-order Jahn–Teller effect common to other highly distorted μ-alkyne complexes previously analysed. A substantially different description of the nature and occupancies of the HOMO and LUMO are found for $[W_2(\eta\text{-}C_5H_5)_2Br_4]$ in the perpendicular-bridging geometry, together with a reasonable energy separation between them. Furthermore, alkyne rotation is not of the correct symmetry to allow intermixing between the HOMO and LUMO. Instead, a rehybridisation of the $W_2(\eta\text{-}C_5H_4Pr^i)_2Br_4$ frontier orbitals [which arises from a modification of the idealised eclipsed $W_2(\eta\text{-}C_5H_4Pr^i)_2Br_4$ core geometry caused solely by the ground-state steric influence of the bridging ligand] occurs so that the HOMO contains comparable $\delta^*(d_{xy})$ and $\delta(d_{x^2-y^2})$ metal character. This combination of orbital contributions allows the HOMO to remain low in energy as alkyne rotation proceeds and hence a distorted complex results.

Computational Details

Molecular orbital calculations were performed using a modified extended-Hückel method employing weighted H_{ij} values.[13] The atomic coordinates were idealised to C_{2h} (for **A**) or C_2 symmetry, but unless stated otherwise bond lengths (W–W 2.80, W–Br 1.59, W–Br* 1.69, C_{ac}–C_{ac} 1.40, C–C 1.41 and C–H 1.0 Å) and angles [W–W–Br 100.5, W–W–Br* 100.5 or 122, W–W–(C_5H_5 centroid) 128 and C_{ac}–C_{ac}–H 132°] were taken from the crystal structure of $[W_2(\eta\text{-}C_5H_4Pr^i)_2Br_4(\mu\text{-}C_2Ph_2)]$.[11] The alkyne was allowed to rotate 1.54 Å above the W–W bond. The atomic parameters were taken from previous work.[16]

Acknowledgements

I thank Professors M. L. H. Green (Oxford) and D. M. P. Mingos (Imperial College) for helpful discussions.

References

1 H. W. Steinberg, H. Greenfield, R. A. Friedel, J. Wotiz, H. R. Markby and I. Wender, *J. Am. Chem. Soc.*, 1954, **76**, 1457; W. G. Sly, *J. Am. Chem. Soc.*, 1959, **81**, 18.
2 D. M. Hoffman, R. Hoffmann and C. R. Fisel, *J. Am. Chem. Soc.*, 1982, **104**, 3858.
3 F. A. Cotton and W. T. Hall, *Inorg. Chem.*, 1980, **19**, 2354; M. H. Chisholm, B. W. Eichorn, K. Folting and J. C. Huffman, *Organometallics*, 1989, **8**, 49.
4 (*a*) K. J. Ahmed, M. H. Chisholm, K. Folting and J. C. Huffman, *Organometallics*, 1986, **5**, 2171; (*b*) R. P. Aggarwal, N. G. Connelly, M. C. Crepso, B. J. Dunne, P. M. Hopkins and A. G. Orpen, *J. Chem. Soc., Dalton Trans.*, 1992, 655; (*c*) F. A. Cotton and M. Shang, *Inorg. Chem.*, 1990, **29**, 508.
5 M. J. Calhorda and R. Hoffmann, *Organometallics*, 1986, **5**, 2181.
6 D. L. Thorn and R. Hoffmann, *Inorg. Chem.*, 1978, **17**, 126.
7 F. A. Cotton and X. Feng, *Inorg. Chem.*, 1990, **29**, 3187.
8 T. A. Albright, J. K. Burdett and M.-H. Whangbo, *Orbital Interactions in Chemistry*, Wiley-Interscience, New York, 1985.
9 P. B. Hitchcock, M. F. Lappert and M. J. McGeary, *J. Am. Chem. Soc.*, 1990, **112**, 5658; E. Spaltenstein and J. M. Mayer, *J. Am. Chem. Soc.*, 1991, **113**, 7744.
10 (*a*) M. L. H. Green, J. D. Hubert and P. Mountford, *J. Chem. Soc., Dalton Trans.*, 1990, 3793; (*b*) M. L. H. Green and P. Mountford, *Chem. Soc. Rev.*, 1992, **21**, 29.
11 Q. Feng, M. L. H. Green and P. Mountford, *J. Chem. Soc., Dalton Trans.*, 1992, 2171.
12 S. G. Bott, D. L. Clark, M. L. H. Green and P. Mountford, *J. Chem. Soc., Dalton Trans.*, 1991, 471.
13 R. Hoffmann and W. N. Lipscomb, *J. Chem. Phys.*, 1962, **36**, 2179.
14 M. H. Chisholm, B. K. Conroy, D. L. Clark and J. C. Huffman, *Polyhedron*, 1988, **7**, 903.
15 J. C. Green, M. L. H. Green, P. Mountford and M. J. Parkington, *J. Chem. Soc., Dalton Trans.*, 1990, 3407.
16 R. Hoffmann, *J. Chem. Phys.*, 1963, **39**, 1397; R. H. Summerville and R. Hoffmann, *J. Am. Chem. Soc.*, 1976, **98**, 7240; A. Dedieu, T. A. Albright and R. Hoffmann, *J. Am. Chem. Soc.*, 1979, **101**, 3141.

Received 18*th January* 1994; *Paper* 4/00311J